Geochemistry of volcanic rocks from the Çiçekdağ Ophiolite, Central Anatolia, Turkey, and their inferred tectonic setting within the northern branch of the Neotethyan Ocean

KENAN M. YALINIZ,[1] PETER A. FLOYD[2] & M. CEMAL GÖNCÜOĞLU[3]

[1]*Department of Civil Engineering, Celal Bayar University, Muradiye, Manisa, Turkey (e-mail: mukenan@anet.net.tr)*

[2]*Department of Earth Sciences, University of Keele, Staffordshire, ST5 5BG, UK*

[3]*Department of Geological Engineering, Middle East Technical University, TR-06531 Ankara, Turkey*

Abstract: The Central Anatolian Ophiolites (CAO) comprise a number of little studied Upper Cretaceous ophiolitic bodies that originally represented part of the northern branch of the Neotethyan ocean. The Çiçekdağ Ophiolite (CO) is an dismembered example of this ophiolite group that still retains a partially preserved magmatic pseudostratigraphy. The following units (bottom to top) can be recognized: (1) layered gabbro; (2) isotropic gabbro: (3) plagiogranite; (4) dolerite dyke complex; (5) basaltic volcanic sequence; and (6) a Turonian–Santonian epi-ophiolitic sedimentary cover. The magmatic rock units (gabbro, dolerite and basalt) form part of a dominant comagmatic series of differentiated tholeiites, together with a minor group of primitive unfractionated basalts. The basaltic volcanics mainly consist of pillow lavas with a subordinate amount of massive lavas and rare basaltic breccias. Petrographic data from the least altered pillow lavas indicate that they were originally olivine-poor, plagioclase–clinopyroxene phyric tholeiites. Immobile trace element data from the basalt lavas and dolerite dykes show a strong subduction-related chemical signature. Relative to N-mid-ocean ridge basalt the Çiçekdağ basaltic rocks (allowing for the effects of alteration) have typical suprasubduction zone features with similarities to the Izu-Bonin Arc, i.e. enriched in most large-ion lithophile elements, depleted in high field strength elements and exhibiting depleted light rare earth element patterns. The geochemical characteristics are similar to other eastern Mediterranean Neotethyan SSZ-type ophiolites and suggest that the CO oceanic crust was generated by partial melting of already depleted oceanic lithosphere within the northern branch of the Neotethyan ocean. The Çiçekdağ body, along with the other fragmented CAO, is thus representative of the Late Cretaceous development of new oceanic lithosphere within an older oceanic realm.

Turkey occupies a critical segment in the Alpine–Himalayan orogenic system where remnants of both the Palaeotethyan and Neotethyan ocean basins crop out along broadly linear tectonic belts. Turkey is divided into three main east–west trending belts of separate ocean basins (Şengör & Yılmaz 1981): (1) a northern belt representing remnants of an Intra-Pontide ocean; (2) a median belt representing allochthonous units derived from the Vardar–İzmir–Ankara–Erzincan (VIAE) ocean [although Görür *et al.* (1984) also consider a separate derivation for the Inner Tauride Belt]; and (3) a southern belt, variably called the Peri-Arabic Belt or southern Neotethyan ocean (Şengör & Yılmaz 1981) (Fig. 1, inset a).

Most of the ophiolites occurring in these belts have been studied to varying degrees, although the isolated outcrops of allochthonous ophiolitic rocks (termed the Central Anatolian Ophiolites; CAO) found in the Central Anatolian Crystalline Complex (CACC) have received little attention until now. The CACC represents the northern passive margin of the Mesozoic Tauride–Anatolide Platform that faced the VIAE ocean (Göncüoğlu 1986; Göncüoğlu *et al.* 1991) (Fig. 1). The CAO are significant in that they were initially generated within the VIAE ocean and emplaced southwards onto the CACC (Yalınız & Göncüoğlu 1998). The majority of these ophiolites are tectonically dismembered, although stratigraphic reconstruction reveals that they originally represented a complete ophiolitic sequence (Yalınız & Göncüoğlu 1998) (Fig. 1, inset b).

In terms of the pseudostratigraphic relationship of the magmatic units and their chemical designation, the CAO exhibit a suprasubduction zone (SSZ) character within the VIAE segment of the Neotethys (Yalınız 1996; Yalınız &

From: Bozkurt, E., Winchester, J. A. & Piper, J. D. A. (eds) *Tectonics and Magmatism in Turkey and the Surrounding Area.* Geological Society, London, Special Publications, **173**, 203–218. 1-86239-064-9/00/$15.00

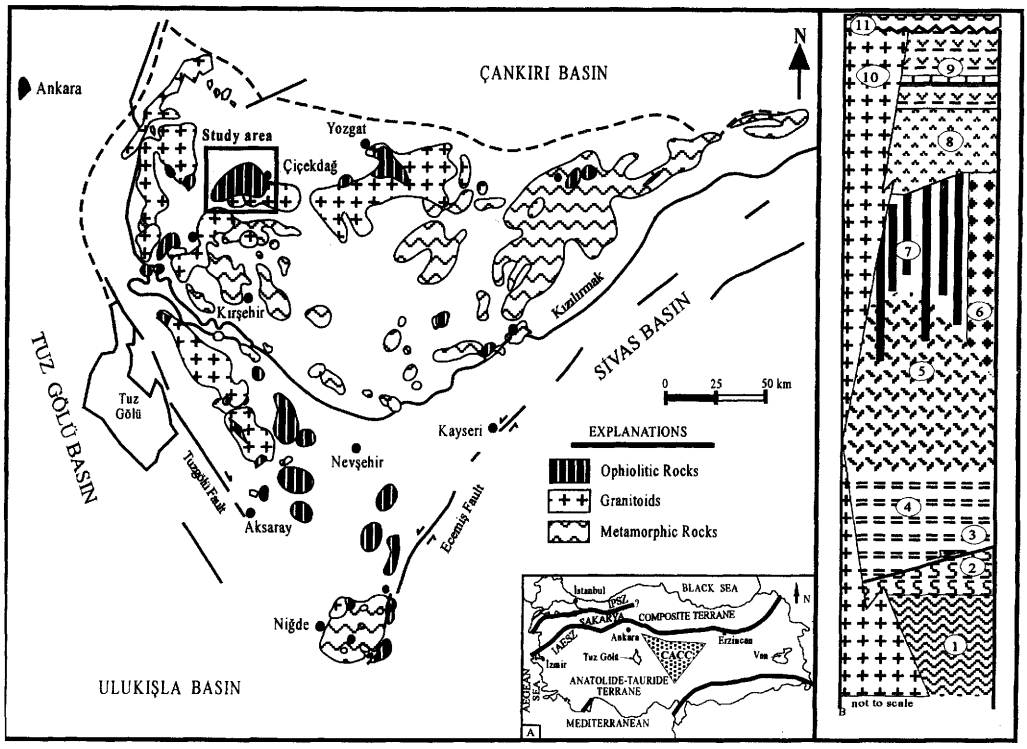

Fig. 1. Generalized geological map of the Central Anatolian Crystalline Complex and the location of the Çiçekdağ Ophiolite. (**a**) Neotethyan suture map of Turkey and the location of the Central Anatolian Crystalline Complex (CACC); IPSC, Intra-Pontide Suture Zone; IAESZ, İzmir–Ankara–Erzincan Suture Zone; SEASZ, Southeast Anatolian Suture Zone. (**b**) Simplified columnar section of the Çiçekdağ Ophiolite: 1, Central Anatolian Metamorphics; 2, metamorphic ophiolite-bearing olistostrome; 3, thrust boundary; 4, layered gabbro; 5, isotropic gabbro; 6, plagiogranites; 7, dyke complex; 8, massive and pillow lavas; 9, epiophiolitic sediments and lavas; 10, granitoids; 11, Lower Tertiary cover sediments.

Göncüoğlu 1998; Yalınız *et al.* 1996; Floyd *et al.* 1998*a*).

Objectives

The Çiçekdağ Ophiolite (CO) is one of the most complete and best exposed of the CAO bodies. Although it has not been studied in detail, little geochemical data being available, its general character invites comparison with other better known CAO, such as the Sarıkaraman Ophiolite (SO). New and extensive geochemical data on the least altered volcanic rocks of the CO are presented here. The purpose of this study is to describe the compositional features of the volcanic rocks of the CO as a basis for determining their original tectonic setting and a comparison with other better known SSZ-type Central Anatolian ophiolites. A further aim is to discuss the genesis and the palaeotectonic setting of the CO within the VIAE ocean to provide a fuller picture for the geodynamic evolution of the northern branch of the Neotethys.

Distribution of rock types and stratigraphy

The CO tectonically overlies the CACC basement along a moderately steep northward dipping thrust just to the south of the Çiçekdağ Massif. Previous field studies in the Çiçekdağ area were mainly carried out by Ketin (1959), Erdoğan *et al.* (1996) and Yılmaz-Şahin & Boztuğ (1997). Typical ophiolitic sequences are exposed around Akçakent, in the core of a roughly north–south trending antiform in the Çiçekdağ region (Fig. 2). Well-preserved and unfaulted successions are rare, although the section along the Akçakent–Kilimli road exhibits much of the original structure.

The CO pseudostratigraphy consists (from top to bottom) of mainly pink pelagic cherty

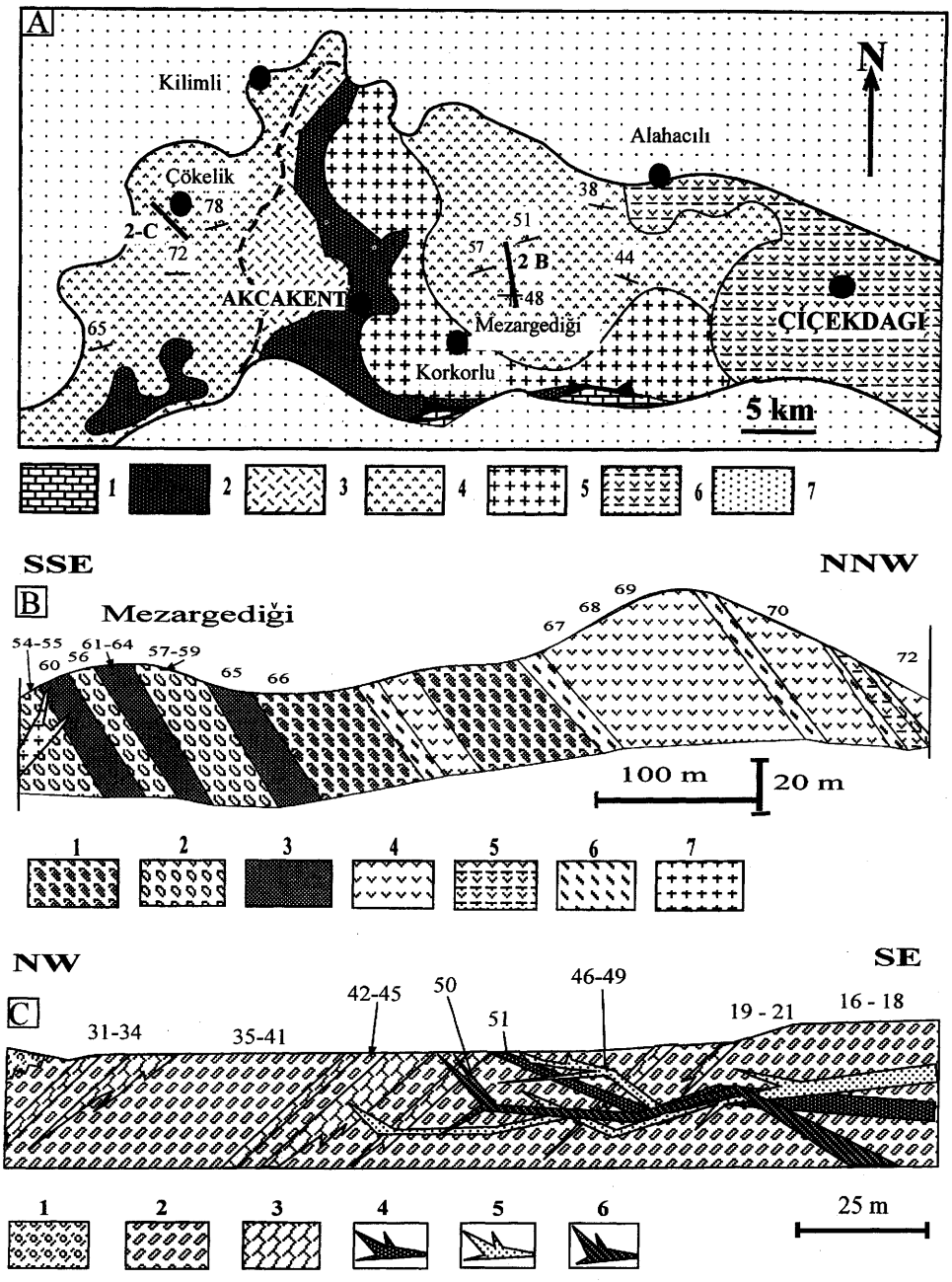

Fig. 2. (**a**) Simplified geological map of the Çiçekdağ Ophiolite and surrounding area. 1, Central Anatolian Metamorphics; 2, layered and isotropic gabbros; 3, dyke complex; 4, lavas and epi-ophiolitic sediments; 5, granitoids; 6, Eocene cover units; 7, Neogene continental clastics; 8, locations of geological cross-sections (S-1, Çökelik section; S-2, Mezargediği section). (**b**) Generalized geological cross-section from the Mezargediği Pass; 1, spherulitic pillow lava; 2, pillow lava; 3, pillow breccia; 4, massive lava; 5, lavas interlayered with sediments; 6, pelagic sediments; 7, feldspathoidal granitoids; 8, sample locations (numbers correspond to samples listed in Table 1). (**c**) Generalized geological cross-section from Çökelik village; 1, Tertiary cover; 2, pillow lavas and volcaniclastics; 3, pelagic sediments; 4, Group III dykes; 5, Group II dykes; 6, Group I dykes; 7, sample locations (numbers correspond to samples listed in Table 1).

limestone and pillow intercalations of Turonian–Santonian age (Erdoğan *et al.* 1996), pillowed and massive basalts with basaltic breccias, sheeted dyke complex, isotropic to layered gabbros and rare associated plagiogranites (Fig. 1, inset b). The lavas, which exhibit typical pillow structures, are best developed at the top of the volcanic sequence where volcanoclastic intercalations are also present. Massive basaltic flows, ranging in thickness from *c.* 1 to 3 m, are also present. The volcanic–volcanosedimentary successions are known as the Çökelik Volcanics (Erdoğan *et al.* 1996), which outcrop on the flanks of the antiformal structure. The areas immediately to the northeast of Korkorlu village and southwest of Çökelik village on the western flank, and the Mezargediği area on the eastern flank of the antiformal structure provide well-exposed sections through the basaltic extrusives. Due to the rarity of volcanic rock exposures in the vicinity of Çiçekdağ, these locations are particularly important and were chosen for detailed sampling (Fig. 2a and b). The sheeted dyke complex is poorly exposed relative to the gabbros but locally contains plagiogranite dykes. The gabbroic sequence is mainly composed of isotropic gabbros and subordinate layered gabbros. The ultramafic part of the ophiolite sequence is not observed in the Çiçekdağ area.

The ophiolitic succession is intruded by early monzogranitic, and later syenitic, intrusions. To the east and northeast of Korkorlu village, gabbroic and basaltic rocks are found as roof pendants within the granitoids. Dykes of feldspathoidal syenites are the last products of the Late Cretaceous collision-type felsic magmatism and cross-cut the volcanic carapace. The earliest fossiliferous cover sediments in the Çiçekdağ region are Lutetian in age (Ketin 1959).

Petrography

The basaltic rocks of the CO are weakly to strongly phyric, with plagioclase and subordinate clinopyroxene as phenocryst phases set in a variably quenched matrix of serrated plagioclase microlites, variolitic fans of crystallites and an opaque matrix. In the Çökelik area, basalts intercalated with the sediments higher in the ophiolite sequence are distinguished from the lower flows by the presence of sparse 'olivine' phenocrysts, which are usually pseudomorphosed by orange-red calcite and hematite in these pervasively altered rocks.

Basaltic samples are all hydrothermally altered to varying degrees. In many sections, the effects of alteration are so intense that primary mineral phases and magmatic textures are strongly overprinted by secondary minerals. As well as the matrix, secondary minerals are also abundant in vesicles, veins and pillow interstices, and include albite, chlorite, epidote, quartz, calcite, actinolite and iron oxides. Fresh clinopyroxene phenocrysts are the only relict igneous phase, although they occasionally show marginal alteration to actinolite. Actinolitic amphibole crystals are also identified as needles in the groundmass. Throughout the Çiçekdağ basaltic lavas, plagioclase laths and phenocrysts are mostly pseudomorphosed by albite. Chlorite commonly occurs in the groundmass of these lavas and also as massive, radiating fibrous aggregates infilling vesicles and veinlets. Epidote is found in vesicles at the margins of lava flows, along the walls of fractures and in veinlets. Where it occurs as a vesicle infill, it forms fan-shaped crystal aggregates often reaching 2–3 cm in diameter, commonly surrounded by subhedral quartz crystals which line the vesicles. Quartz is generally deposited together with epidote and forms a vesicle infill. Calcite is much less abundant than chlorite, epidote and quartz in the Çiçekdağ lavas, but similarly occurs in rock spaces rather than replacing previous minerals. Pillow breccias show similar petrography and textures.

The dykes display an equigranular texture, are medium to fine grained, and are characterized by ophitic, subophitic and intergranular textures. They are mostly aphyric to sparsely plagioclase–phyric dolerites. Although the primary igneous mineralogy of the dykes consists of clinopyroxene, calcic plagioclase and opaque minerals, most of these are replaced by a greenschist facies assemblage made up of actinolite, chlorite, epidote, plagioclase, quartz, sphene and secondary Fe–Ti oxides and hydroxides. Rare core relicts of clinopyroxene are also locally identified at the base of the sheeted dyke complex. Most dykes retain their primary igneous textures but there are some that are more severely altered to equigranular textured quartz- and epidote-rich epidosites. These are often green coloured compared to the more normal grey dykes that are usually characterized by dominantly albite–actinolite–chlorite assemblages.

Sampling and analytical methods

Sixty-three samples were collected from basaltic lavas and dykes, many selected from the Mezarğediği and Çökelik traverses (see location and relative sampling positions in Fig. 2). Mafic samples were taken from the crystalline

Table 1. *Representative chemical analyses of basaltic lavas and dykes from the Çiçekdağ Ophiolite*

Sample	**C-6**	**C-9A**	**C-10A**	**C-10B**	**C-11**	**C-66**	**C-76**	**C-77**	**C-78**	**C-79**	**C-31**	**C-32**	**C-33**	**C-34**	**C-35**	**C-36**	**C-37**	**C-39**	**C-40**	**C-41**	**C-42**
Rock type*	p.lava	p.lava	p.lava	p.lava	p.lava	p.lava	p.lava	p.lava	p.lava	p.lava	p.lava	p.lava	p.lava	p.lava	p.lava	p.lava	p.lava	p.lava	p.lava	p.lava	p.lava
Major oxides (wt%)																					
SiO_2	53.12	53.72	51.59	57.12	47.36	48.64	52.41	52.88	49.37	50.52	50.59	51.06	44.43	45.34	49.41	45.27	56.45	41.75	43.38	51.78	52.10
TiO_2	1.39	0.44	1.20	1.08	0.76	0.67	0.96	0.81	0.59	0.65	0.44	0.42	0.41	0.41	0.44	0.46	0.36	0.47	0.46	1.18	1.25
Al_2O_3	16.63	13.43	15.91	14.21	14.03	14.04	15.44	15.45	15.43	15.22	14.60	14.07	12.73	13.12	14.41	13.69	13.11	14.30	15.27	15.40	15.84
Fe_2O_3t	12.31	9.85	15.39	12.47	12.10	10.34	9.77	9.49	10.90	10.00	10.34	10.03	8.56	9.20	10.54	9.26	7.77	10.30	11.02	9.92	10.34
MnO	0.26	0.18	0.20	0.16	0.21	0.20	0.23	0.12	0.18	0.15	0.14	0.16	0.18	0.19	0.13	0.16	0.09	0.18	0.17	0.17	0.17
M_gO	3.90	8.96	5.43	3.25	6.64	10.21	5.90	4.83	6.48	7.57	7.84	7.60	4.67	4.93	8.37	3.80	1.24	9.29	10.19	5.72	4.69
CaO	7.55	5.92	2.53	2.82	5.65	11.09	7.69	9.84	9.18	8.53	5.48	9.11	12.37	10.93	5.07	11.01	7.53	9.18	6.47	4.32	6.87
Na_2O	3.69	5.05	5.73	7.09	7.14	1.75	4.92	4.17	3.57	3.09	3.29	3.32	4.95	5.00	3.71	5.99	6.99	3.32	3.45	5.27	3.60
K_2O	0.43	0.09	0.17	0.07	0.08	0.32	0.05	0.04	0.99	1.38	0.22	0.20	0.06	0.07	0.19	0.17	0.14	0.11	0.09	0.27	0.19
P_2O_5	0.06	0.04	0.08	0.09	0.05	0.06	0.10	0.10	0.06	0.06	0.03	0.03	0.04	0.03	0.03	0.04	0.06	0.03	0.03	0.09	0.15
LOI	0.81	2.51	1.55	1.35	5.75	2.65	2.41	2.18	3.43	2.88	7.35	3.71	11.90	10.97	7.83	10.26	6.39	10.94	9.31	5.45	4.51
Total	**100.15**	**100.19**	**99.78**	**99.71**	**99.77**	**99.97**	**99.88**	**99.91**	**100.18**	**100.05**	**100.32**	**99.71**	**100.30**	**100.19**	**100.13**	**100.11**	**100.13**	**99.87**	**99.84**	**99.57**	**99.71**
Trace elements (ppm)																					
Ba	73	36	25	76	47	37	25	7	156	87	22	11	15	41	20	20	19	2	27	18	50
Ce(XRF)	3	1	10	3	1	2	2	3	1	1	3	2	1	3	2	1	8	1	2	1	12
Cl	226	1	5	5	3	28	3	3	2	2	4	2	2	1	1	3	2	2	2	1	1
Cr	21	345	24	9	254	531	179	194	182	330	272	220	220	244	245	177	160	240	334	119	77
Cu	89	162	161	170	74	147	112	13	78	94	27	23	86	38	637	52	29	57	85	16	25
Ga	20	10	13	18	15	13	15	15	11	13	13	13	11	10	13	10	8	12	15	15	19
La(XRF)	3	3	1	1	2	2	2	2	1	1	3	1	1	2	2	1	1	1	3	2	3
Nb	2	1	2	2	2	2	2	2	2	0.5	1	2	1	1	2	1	1	1	1	2	2
Nd(XRF)	5	7	15	1	7	4	6	7	5	1	2	1	7	2	13	2	16	6	13	7	17
Ni	7	55	17	18	70	165	47	47	66	95	53	59	47	52	60	32	52	62	60	28	27
Pb	75	9	9	4	15	8	6	10	10	6	2	4	5	4	2	3	3	1	1	1	4
Rb	17	2	2	5	3	8	1	1	21	24	5	5	3	2	4	3	4	2	2	4	3
S	210	1	2	19	10	47	1	3	2	2	22	14	29	26	32	63	35	26	27	3	1
Sr	190	92	66	134	108	72	188	151	203	164	135	160	72	76	110	101	49	154	160	145	176
V	301	281	576	648	433	292	330	298	296	293	371	312	319	311	377	367	119	373	389	286	272
Y	25	12	23	28	17	20	23	19	14	15	11	11	9	8	11	13	7	12	11	22	26
Zn	195	68	80	135	130	92	83	59	64	109	71	70	71	71	74	64	67	73	80	82	86
Zr	48	20	43	47	32	39	51	44	25	33	14	14	12	12	14	15	13	15	15	48	59

Table 1. *Continued*

Sample	**C-43**	**C-44A**	**C-44B**	**C-45**	**C-54**	**C-55**	**C-56**	**C-57**	**C-58**	**C-59**	**C-67**	**C-68**	**C-69**	**C-70**	**C-72**	**C-13**	**C-16**	**C-17**	**C-18**	**C-19**	**C-21**
Rock type*	p.lava	p.lava	p.lava	p.lava	m.lava	m.lava	m.lava	m.lava	m.lava	m.lava	m.lava	m.lava	m.lava	m.lava	m.lava	breccia	breccia	breccia	breccia	breccia	breccia
Major oxides (wt%)																					
SiO_2	51.21	52.38	55.64	51.98	49.52	53.38	54.30	54.85	52.32	53.04	53.95	54.56	50.05	50.85	51.01	54.01	45.45	51.19	49.99	40.67	48.04
TiO_2	0.46	0.40	0.99	1.26	1.09	0.40	0.65	1.05	0.77	0.83	0.62	0.55	0.80	0.78	0.53	1.21	1.06	1.32	0.66	0.84	0.56
Al_2O_3	14.50	12.04	13.31	16.90	13.65	11.64	14.14	14.47	14.97	14.86	14.79	14.79	15.80	13.81	13.05	16.66	17.93	14.87	15.74	12.18	16.75
Fe_2O_3t	10.09	8.94	13.50	10.71	15.29	8.94	9.32	12.69	9.99	11.70	10.08	9.00	11.86	14.60	10.40	12.09	11.44	12.42	9.11	8.75	8.73
MnO	0.20	0.20	0.15	0.17	0.21	0.20	0.15	0.16	0.14	0.24	0.16	0.16	0.25	0.20	0.23	0.13	0.18	0.14	0.13	0.10	0.15
M_gO	9.28	10.76	5.28	5.65	6.00	10.76	3.77	3.65	4.66	5.98	6.93	5.99	7.74	6.57	10.22	2.00	6.88	3.97	5.74	1.65	8.04
CaO	7.46	9.58	3.35	5.50	4.21	8.69	6.91	4.59	4.69	5.70	5.27	7.49	5.48	7.18	9.07	1.60	12.21	4.76	6.33	16.50	10.56
Na_2O	2.53	2.17	2.53	3.65	5.20	2.06	6.43	6.53	6.19	5.55	4.99	4.22	4.59	3.27	2.60	8.64	2.41	4.20	2.46	6.67	3.41
K_2O	0.08	0.49	0.18	0.36	0.07	0.69	0.13	0.08	0.12	0.23	0.53	1.50	0.15	0.15	0.69	0.20	0.37	0.04	0.18	0.09	0.12
P_2O_5	0.03	0.02	0.10	0.14	0.07	0.02	0.08	0.08	0.07	0.08	0.05	0.05	0.08	0.07	0.05	0.08	0.04	0.13	0.06	0.19	0.05
LOI	4.18	3.06	4.57	3.28	4.12	3.06	3.98	1.58	4.90	1.80	2.30	1.57	2.53	2.36	2.31	1.01	1.88	6.92	9.44	12.68	3.62
Total	**100.02**	**100.04**	**99.60**	**99.60**	**99.43**	**99.84**	**99.86**	**99.73**	**99.82**	**100.01**	**99.67**	**99.88**	**99.33**	**99.84**	**100.16**	**97.63**	**99.85**	**99.96**	**99.84**	**100.32**	**100.03**
Trace elements (ppm)																					
Ba	29	111	52	91	34	98	46	30	39	125	98	262	19	39	116	182	53	17	55	24	42
Ce(XRF)	2	2	7	2	7	1	13	3	2	9	4	7	3	5	4	6	3	5	2	2	1
Cl	1	1	2	1	2	2	1	1	2	201	26	60	28	59	24	5	4	2	3	1	1
Cr	197	519	20	103	9	515	219	17	265	71	128	118	336	259	537	38	127	27	110	242	223
Cu	172	74	112	46	70	75	249	81	256	104	82	143	84	53	14	50	68	45	109	37	61
Ga	14	11	15	22	18	10	14	18	12	14	13	13	16	15	11	13	19	20	12	8	15
La(XRF)	2	2	1	1	2	3	1	1	2	2	1	2	2	1	1	2	1	4	1	1	2
Nb	1	1	3	3	2	2	1	2	0.41	2	2	0.41	2	2	2	2	4	2	1	2	2
Nd(XRF)	6	9	15	13	14	6	22	12	9	12	8	13	8	13	8	11	9	16	3	6	6
Ni	53	120	16	28	21	124	47	17	63	44	46	43	95	83	187	12	54	16	50	85	92
Pb	3	5	3	4	3	7	58	6	25	9	7	8	7	7	11	6	30	2	5	12	3
Rb	2	18	4	5	2	18	3	2	4	7	10	27	3	3	15	6	6	3	8	2	2
S	2	6	13	3	2	3	5	2	17	2	3	26	62	169	2	9	3	23	12	48	20
Sr	148	131	70	169	101	130	115	113	106	138	76	84	28	65	91	124	737	41	34	106	161
V	312	241	322	245	613	232	395	580	443	334	244	286	357	384	266	385	356	451	332	251	228
Y	11	11	28	28	25	11	20	22	19	22	21	19	22	21	14	26	34	31	17	22	15
Zn	73	66	44	88	132	67	79	76	95	106	87	72	100	88	113	52	75	115	72	82	63
Zr	14	19	69	65	43	18	28	42	32	46	41	39	46	45	27	66	77	80	37	52	30

Table 1. *Continued*

Sample	**C-60**	**C-61**	**C-62**	**C-63**	**C-64**	**C-65**	**C-46**	**C-47**	**C-48**	**C-49**	**C-50**	**C-51**	**C-23**	**C-24**	**C-26**	**C-27**	**C-28**	**C-29**	**C-30**
Rock type*	breccia	breccia	breccia	breccia	breccia	breccia	dyke	dyke	dyke	dyke	dyke	dyke	sh.dyke	sh.dyke	sh.dyke	sh.dyke	sh.dyke	sh.dyke	sh.dyke
Major oxides (wt%)																			
SiO_2	0.82	58.27	54.06	57.82	59.06	60.11	48.68	47.45	43.37	45.54	49.66	53.25	59.50	48.06	52.46	51.49	52.74	51.67	46.85
TiO_2	1.42	1.24	1.26	1.28	1.15	1.23	0.64	0.62	0.63	0.66	0.49	1.21	1.43	1.02	0.99	1.01	1.42	0.96	1.17
Al_2O_3	16.84	14.49	15.98	15.63	14.41	15.68	14.53	14.94	15.14	15.09	14.12	14.33	14.82	14.64	15.78	15.86	15.07	15.30	15.57
Fe_2O_3t	3.22	12.38	13.05	12.65	11.59	11.55	10.12	10.10	9.84	9.78	9.45	9.02	10.11	10.70	11.78	11.90	12.96	11.22	11.49
MnO	0.27	0.13	0.17	0.05	0.15	0.10	0.21	0.23	0.26	0.19	0.15	0.14	0.33	0.34	0.32	0.32	0.30	0.33	0.34
M_gO	4.88	2.08	2.89	0.56	2.33	1.02	8.96	8.84	8.78	8.65	8.04	3.14	3.43	5.78	6.24	7.43	6.04	7.02	6.54
CaO	2.21	2.48	2.54	1.82	2.58	1.50	5.00	5.32	7.64	6.89	8.36	6.34	1.45	6.70	3.19	1.48	2.57	3.49	6.46
Na_2O	6.86	7.90	7.58	9.35	7.73	7.62	3.28	3.56	3.83	3.64	2.99	7.37	6.14	4.96	5.45	5.33	4.96	4.57	5.19
K_2O	0.16	0.12	0.30	0.08	0.20	0.18	0.04	0.04	0.05	0.11	0.08	0.05	0.01	0.04	0.03	0.09	0.05	0.06	0.01
P_2O_5	0.05	0.12	0.10	0.15	0.10	0.09	0.05	0.05	0.05	0.06	0.03	0.10	0.32	0.07	0.08	0.14	0.13	0.07	0.09
LOI	2.40	0.85	1.48	0.31	0.76	0.43	8.45	8.63	10.08	9.57	6.28	5.18	2.61	7.60	3.64	3.99	3.62	5.13	6.45
Total	**99.13**	**100.06**	**99.41**	**99.70**	**100.06**	**99.51**	**99.96**	**99.78**	**99.67**	**100.18**	**99.65**	**100.13**	**100.15**	**99.91**	**99.96**	**99.04**	**99.86**	**99.82**	**100.16**
Trace elements (ppm)																			
Ba	113	56	91	64	156	150	14	19	15	17	9	10	25	33	14	29	30	31	16
Ce(XRF)	5	6	5	5	2	2	1	3	2	2	3	5	15	2	3	7	9	18	11
Cl	33	18	338	154	2	5	1	3	1	1	1	52	18	8	5	2	93	80	1
Cr	5	18	28	12	27	52	543	453	467	423	201	56	6	57	50	37	25	62	48
Cu	39	14	25	21	28	69	133	188	328	68	194	9	200	21	48	16	52	48	16
Ga	22	14	16	12	13	11	14	13	12	14	13	12	17	15	16	14	17	16	17
La(XRF)	3	2	2	1	1	1	2	3	1	1	1	4	1	1	2	1	2	3	1
Nb	2	3	2	3	2	2	2	1	1	2	1	2	0.68	1	2	2	2	2	2
Nd(XRF)	8	6	9	14	3	10	4	11	7	8	2	6	18	4	9	13	16	22	16
Ni	18	13	18	14	18	13	172	147	145	145	59	21	4	26	23	23	17	23	37
Pb	4	5	48	5	2	9	1	1	1	1	2	2	4	8	1	1	2	1	5
Rb	5	3	12	2	6	5	1	2	1	2	1	2	0.3	2	1	2	2	2	2
S	2	9	9	8	39	21	16	14	16	14	21	5	66	141	100	990	319	149	22
Sr	77	92	88	75	143	127	127	135	143	120	148	74	35	79	78	68	69	74	64
V	354	447	376	377	369	430	266	254	237	306	324	224	118	449	375	426	455	430	367
Y	21	29	25	35	30	29	13	13	14	17	10	23	35	22	22	24	33	20	28
Zn	115	54	90	25	54	50	72	73	75	76	75	55	228	171	199	236	394	191	268
Zr	74	65	65	67	62	64	37	37	38	40	14	55	96	41	44	47	69	42	54

* p.lava, Pillow lava; m.lava, massive lava; breccia, pillow lava breccia; dyke, individual dykes cross-cutting lavas; sh.dyke, sheeted dyke complex.

Table 2. *Additional chemical data on Çiçekdağ basaltic rocks*

Sample	**C-58**	**C-68**	**C-79**	**C-23**
Rock type	Massive lava	Massive lava	Pillow lava	Sheeted dyke
Incompatible elements (ppm)				
Os	3.08	2.67	0.97	0.13
Hf	0.73	0.83	0.73	1.08
Sc	38.77	38.33	46.67	42.40
Ta	0.03	0.04	0.04	0.05
Th	0.06	0.11	0.07	0.07
U	0.11	0.20	0.12	0.15
Rare earth elements (ppm)				
La	1.59	1.47	1.18	1.43
Ce	3.63	3.94	3.39	4.30
Pr	0.65	0.67	0.57	0.76
Nd	3.64	3.73	3.17	4.39
Sm	1.27	1.34	1.13	1.63
Eu	0.50	0.56	0.45	0.60
Gd	1.83	1.97	1.64	2.42
Tb	0.34	0.37	0.31	0.45
Dy	2.22	2.41	2.05	2.96
Ho	0.49	0.54	0.45	0.65
Er	1.46	1.60	1.32	1.87
Tm	0.25	0.26	0.22	0.32
Yb	1.50	1.61	1.35	1.92
Lu	0.24	0.26	0.22	0.31

interiors of pillows, pillow breccias, massive lavas and dykes, and selected in order to minimize the effect of vesiculation, alteration and weathering. All samples were analysed for major and selected trace elements, and a subset of four samples for rare earth element (REE), and Hf, Ta, Th and U (Tables 1 and 2). Analysis for major oxides and most trace elements were determined on an ARL 8420 X-ray fluorescence spectrometer (Department of Earth Sciences, University of Keele, UK) calibrated against both international and internal Keele standards of appropriate composition, whereas the REE etc. were determined by instrumental neutron activation analysis (Activation Laboratories Ltd, Canada). Details of methods, accuracy and precision are given in Floyd & Castillo (1992).

Chemical discrimination

As outlined above, all the basaltic lavas and dykes in the CO have undergone greenschist facies alteration and metamorphism. Thus, for chemical discrimination of the volcanics, only elements that are immobile during alteration should be used. There is general agreement that the high field strength elements (HFSE: P, Ti, Y, Zr, Nb, Hf, Ta; Saunders *et al.* 1980), Th (Wood *et al.* 1979), the transition metals (Sc, V, Cr, Ni) and REE are essentially immobile during all but the most severe seafloor or hydrothermal alteration (e.g. Pearce 1975; Shervais 1982). SiO_2 and most large-ion lithophile elements (LILE: Na, K, Cs, Rb, Ba, Sr) are almost certainly mobile under these alteration conditions (Smith & Smith 1976; Coish 1977; Humphris & Thompson 1978*a*, *b*). Thus, chemical discrimination mainly relies on the HFSE and REE, which tend to be the least mobile in aqueous fluids.

Geochemistry

General features

On the basis of their Nb/Y ratios (Winchester & Floyd 1977), all the mafic samples are tholeiitic (Nb/Y = 0.04–0.20) with generally low HFSE contents (Table 1). Metabasaltic lavas from the Mezargediği and Çökelik traverses have overlapping compositions in terms of incompatible element abundances, similar Zr/Y and Zr/Ti ratios, and depleted REE patterns. These features suggest that they represent a similar lava sequence, possibly related to a single chemical group, but now separated by tectonic dismemberment. However, direct chemical correlation is not possible between the two lava sequences throughout, as two characteristics found in the Çökelik traverse are missing in the Mezargediği

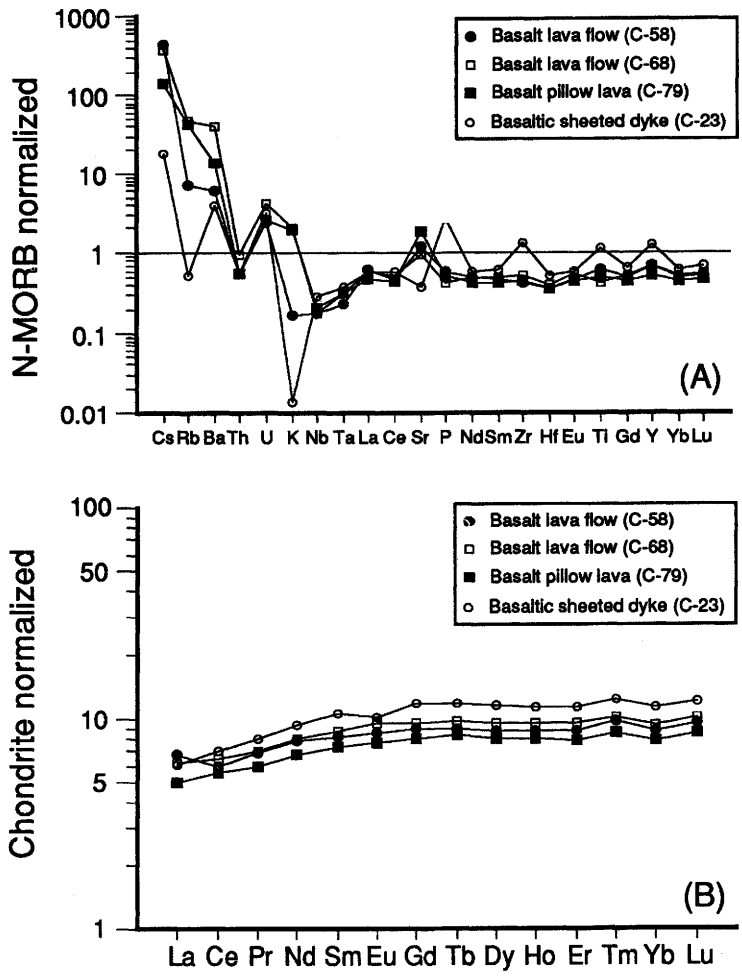

Fig. 3. (**a**) N-MORB normalized multi-element diagram for Çiçekdağ basalts showing HFSE element depletion and LILE enrichment. (**b**) Chondrite-normalized REE patterns of Çiçekdağ basalts showing light REE depletion. Normalization factors from Sun & McDonough (1989).

traverse. In particular, the former sequence contains numerous feeder dykes towards the base and a set of primitive lavas with low Zr and Y contents that are missing from the Mezargediği sequence. On the grounds that the lower volcanic portions of an ophiolite should contain a greater density of feeder dykes than the upper, it is suggested that the Çökelik sequence records a generally lower volcanic section than the Mezargediği sequence.

Normalized patterns for incompatible elements and REE (Fig. 3) illustrate a number of features typical of the CO. All basaltic samples show broadly parallel and depleted light REE patterns with (La/Yb)N of *c.* 0.6, suggesting that the samples plotted are probably related by simple fractionation. Relative to N-mid-ocean ridge basalt (MORB), the normalized incompatible element patterns show the depleted HFSE and enriched LILE features of SSZ ophiolites, although the later variable abundances (apart from Th) are largely governed by alteration effects.

Internal variation

Samples from the lavas and dykes of the Mezargediği and Çökelik traverses, and isolated locations elsewhere, show internal variation that is largely governed by fractional crystallization. Using Zr as a fractionation index, increasing FeO^*/MgO (Fig. 4a) and decreasing Cr (Fig.

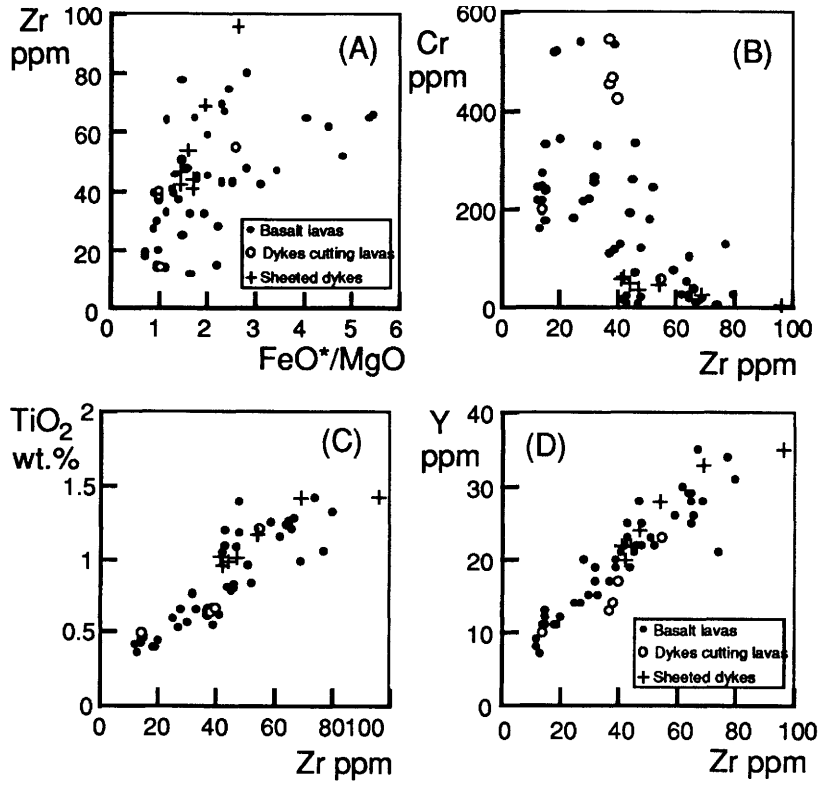

Fig. 4. Chemical diagrams illustrating internal variation for Çiçekdağ lavas and dykes. (**a**) and (**b**), Effects of mafic fractionation; (**c**) and (**d**), linear covariance suggests a single comagmatic suite for the basalts.

4b) implies mafic fractionation, as indicated by the observed relict phenocryst phases. Some of the scatter here is the consequence of alteration, whereas the covariance of immobile elements (Fig. 4c and d) indicate that all the samples probably represent a single, fractionated, comagmatic chemical group. The very low Zr (< 20 ppm) and Y (*c.* 10 ppm) set of samples, however, might be a different chemical group from the rest, especially in view of their position in the Çökelik traverse magmatic stratigraphy (see below).

Chemostratigraphy

Systematic sampling along the Mezargediği and Çökelik traverses allows some monitoring of chemical variability with height in the volcanic portion of the CO. Due to tectonic dismemberment, stratigraphic height is only relative, being measured from the arbitrary base of the traverse in both cases. As seen in Fig. 5, the basal part of each traverse is highly variable in terms of the elements plotted, whereas the uppermost

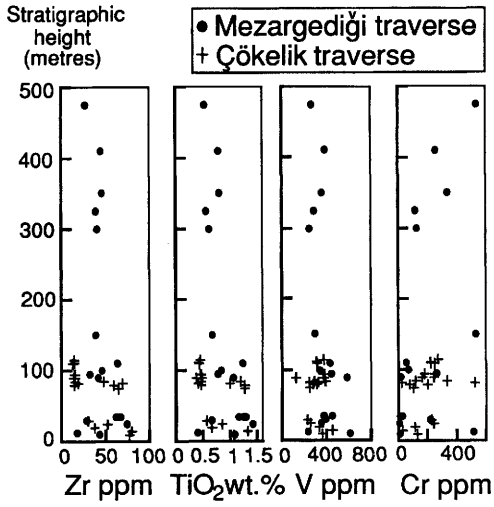

Fig. 5. Chemical variation with height in the Çiçekdağ lavas. Height is relative and arbitrary starting at the base of the traverse in both the Mezargediği and Çökelik sequences.

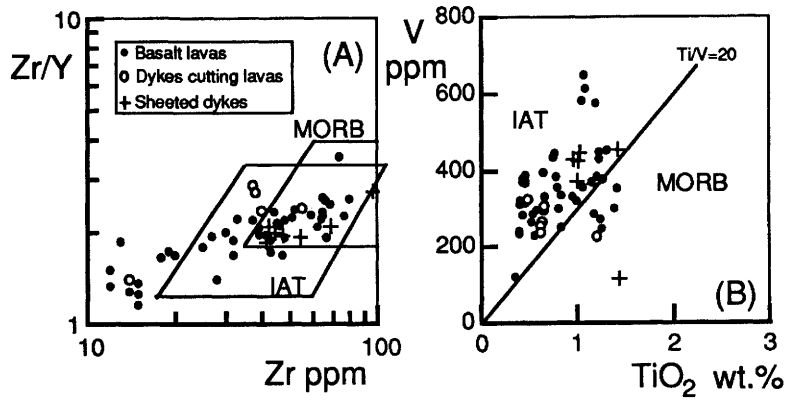

Fig. 6. Discrimination of tectonic setting using chemical parameters. (**a**) Zr/Y v. Zr [after Pearce & Norry (1979)]; (**b**) V v. TiO_2 [after Shervais (1982)].

portion is more 'steady state', although this effect may be more apparent than real (fewer samples were collected here). The chemical stratigraphy is interpreted here in terms of the periodic tapping of a well-fractionated magma chamber which, in the light of the similarity in composition of the two traverses, might be the same ponded magma body. However, this simple picture must be modified to allow for the presence of the primitive lavas with low HFSE contents at *c.* 80–110 m from the base in the Çökelik traverse. It is suggested that these lavas represent an influx of pristine, largely unfractionated, melt derived from another source which were not involved with the main fractionated magma chamber.

In general, the similarity of basaltic compositions indicate that open-system processes were limited throughout the section available and only one (or possibility two) chemical groups were involved.

Tectonic discrimination

A number of plots can be used to discriminate the provenance of the CO basalt samples (Fig. 6). Despite some compositional overlap with the island arc tholeiites (IAT) and MORB designated fields, most samples clearly fall within the former, especially in the TiO_2 v. V diagram. It is also apparent that, relative to the majority of the samples, the very low Zr–Y Çökelik samples plot outside the IAT field (Fig. 6), again emphasizing their different nature and origin.

N-MORB normalized multi-element plots for the CO basalts (Fig. 3) show the depletion of HFSE (Nb, Ta, Zr, Hf, Ti, P; generally < 1) together with the relative LILE (K, Ba, Sr, Rb, Th) enrichment features characteristic of subduction-related arc magmas (e.g. Wood *et al.* 1979; Wood 1980; Pearce 1982; Pearce & Parkinson 1993; Pearce *et al.* 1984). Within the generally mobile LILE group, Th is a relatively stable and reliable indicator, whose enrichment relative to other incompatible elements (especially Nb–Ta) is taken to represent the subduction zone component (e.g. Wood *et al.* 1979; Pearce 1983). This feature is attributed to the modification of the mantle source region of the Çiçekdağ basalts by a 'subduction component', i.e. metasomatism by aqueous fluids derived from the underlying subducting slab (e.g. Pearce 1982; Pearce *et al.* 1984; Hawkesworth *et al.* 1977, 1993; Saunders & Tarney 1984; McCulloch & Gamble 1991). In general, the CO has all the features typical of suprasubduction oceanic crust (Pearce *et al.* 1984).

Normalized REE patterns (Fig. 3) for basalts do not generally make good discriminants due to similar patterns being generated in different environments. For example, both MORB and back-arc basin basalts (BABB) are characterized by patterns that display slight light REE depletion relative to the heavy REE and are generally enriched 10–20 times relative to chondrite. Distinguishing between basalts formed in these two eruptive settings is therefore not possible solely on the basis of REE patterns. REE patterns of most IAT also display a large degree of overlap with MORB-type patterns, although the former can exhibit varying degrees of light REE enrichment and depletion (e.g. White & Patchett 1984; Brouxel *et al.* 1989). Since normal IAT may exhibit variable light REE patterns from extremely depleted (e.g. Mariana forearc; Hickey & Frey 1981; Crawford *et al.* 1986) to substantially flat (e.g. Tonga–Kermadec; Ewart *et al.* 1977: Yap Trench;

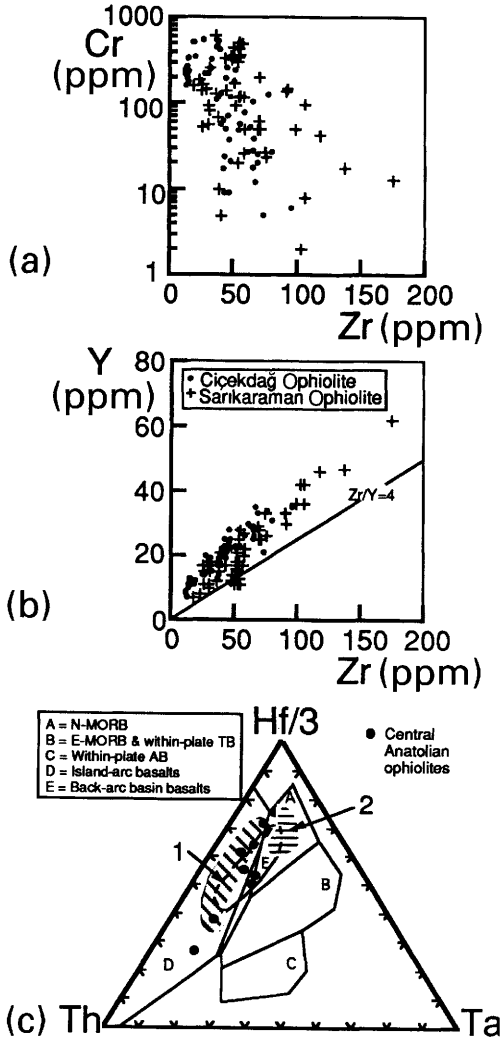

Fig. 7. (**a**) and (**b**) Chemical comparisons of Çiçekdağ and Sarıkaraman ophiolitic basalts; (**c**) Comparison of Çiçekdağ and Sarıkaraman basalts with SSZ-type eastern Mediterranean ophiolites (area 1) and MORB-type western Mediterranean ophiolites (area 2). Comparison data selected from the Tethyan ophiolite literature (e.g. Pearce *et al.* 1984). Discrimination fields after Wood (1980).

Beccaluval & Serri 1988) to slightly enriched (e.g. Aleutians and Sunda; Kay 1977), it follows that the components added to IAT mantle sources generally carry minor light REE in addition to K, Rb, Ba, Sr, Th, U, Cs and H_2O. However, strongly REE-depleted tholeiites are generally interpreted as a product of immature island arcs (Crawford *et al.* 1986; Brouxel *et al.* 1989). It is suggested that the REE patterns shown by the CO can best be matched with arc basalts similar to those found in immature island-arc sequences such as the Izu-Bonin Arc.

Comparison with the Sarıkaraman and other Neotethyan ophiolites

The CO and the Sarıkaraman Ophiolite (SO) are representative members of the CAO (Göncüoğlu *et al.* 1991). Both are characterized by the lack of ultramafic rocks in direct contact with the rest of the ophiolitic slab. The lowest section of the CO is composed of layered gabbros, whereas isotropic gabbros are found at the base of the SO (Yalınız *et al.* 1996). The SO is remarkable in displaying a high portion of the plagiogranite suite (Floyd *et al.* 1998*a*) and a late set of isolated dykes (Yalınız *et al.* 1996). Neither of these features are as well developed in the CO, nor exposed to the same degree. Both ophiolites are overlain by a sequence of Lower Turonian–Campanian pelagic sediments and are also intruded by Upper Cretaceous–Lower Palaeocene granitoids (Göncüoğlu *et al.* 1991; Yalınız *et al.* 1996).

It has previously been shown that the volcanic section of the SO exhibits typical SSZ characteristics similar to other Neotethyan ophiolites (Yalınız *et al.* 1996), including the CO. The CO closely matches the variation shown by the SO but lacks the extensive degree of chemical evolution (Fig. 7); the lavas sampled are less chemically evolved. A significant difference is also exhibited by the latter cross-cutting dolerite dykes of the SO which has a MORB-like affinity (Yalınız *et al.* 1996). In general, minor differences are apparent in their stratigraphy, although overall the basalts have a similar chemistry and formation age.

The CAO are also part of a long chain of Tethyan ophiolites that extend from the western Mediterranean to the Far East. Petrological and geochemical studies have shown that there are important differences along the Tethyan ophiolitic belt. Several workers have divided the Tethyan ophiolites into two groups: (1) Jurassic ophiolites in the western and central area (Alps, Appennines, Carpathians, Dinarides, Hellenides) which display MORB affinities; and (2) Cretaceous ophiolites at the eastern Mediterranean end (Troodos, Semail, Baer-Bassit, Hatay) which exhibit SSZ features (e.g. Pearce *et al.* 1984). Since the chemical signature of the Cretaceous Çiçekdağ lavas also indicate that they were generated in a SSZ, this ophiolite can be fitted into the regional tectonic framework, displaying a similar tectonic setting to other late

Cretaceous Neotethyan ophiolites in the eastern Mediterranean area (Fig. 7).

Genesis and emplacement of SSZ-type Central Anatolian ophiolites

The geodynamic evolution of the İzmir–Ankara branch of Neotethys has been the topic of copious studies (e.g. Robertson & Dixon 1984; Tüysüz *et al.* 1995; Okay *et al.* 1998). All of these studies are based mainly on very general approaches and broadly consider the geological–geochemical aspects. Any model explaining the tectonic evolution of the İzmir–Ankara branch of Neotethys must be consistent with the following local and regional constraints. Firstly, the stratigraphic succession in the Central Anatolian Metamorphic Complex is almost identical with that of the less metamorphosed Palaeozoic–Mesozoic platform margin sequences of the Taurides–Anatolides (Göncüoğlu *et al.* 1991). It differs from the later only by a complex high-temperature–low-pressure (HT–LP) metamorphic overprint and the presence of collision-type magmatism. Secondly, the upper part of the metamorphic succession is represented by an ophiolite-bearing olistostromal complex, representing synorogenic flysch deposition on the platform margin (Göncüoğlu 1981). The ophiolitic knockers within this meta-olistostrome display mainly MORB characteristics with minor ocean island basalt (OIB) and IAT (Floyd *et al.* 1998*b*). Thirdly, the metamorphic rocks are overthrust by dismembered ophiolites with SSZ-type geochemical characteristics akin to other eastern Mediterranean ophiolites (Yalınız *et al.* 1996; Floyd *et al.* 1998*a*, *b*). Structural data clearly indicate an emplacement direction towards the south and southwest. The formation age is early Middle Turonian–Early Santonian, based on palaeontological data from the associated epi-ophiolitic sedimentary rocks (Yalınız *et al.* 1997). The markedly high volume of epiclastic volcanogenic sediments in this succession suggests the involvement of an island arc. Finally, the accretionary wedge complex (the Ankara Mélange) to the north of the CACC, which was formed within the converging İzmir–Ankara branch of Neotethys, contains slivers of ophiolitic rocks dominated by MORB, OIB, and minor IAT compositions, characteristic of forearc accretionary wedge complexes (Floyd 1993; Floyd *et al.* 1998*b*). Associated sediments yield Late Triassic–Early Cretaceous fossils.

These data suggest: (1) the oceanic crust of the İzmir–Ankara branch of Neotethys has been partly consumed along a north dipping intra-oceanic subduction zone (Göncüoğlu *et al.* 1991); and (2) the SSZ-type ophiolitic bodies, observed both as allochthonous thrust sheets on the Taurides–Anatolides and as blocks in the mélange complexes, were generated within the MORB-type old hanging-wall block of the İzmir–Ankara oceanic crust and emplaced southwards onto the Tauride–Anatolide passive margin.

However, oceanic crust formation in a SSZ setting can involve quite different tectonic settings, such as active island arcs, back-arc and forearc basins. Thus, for a better understanding of the evolution of the Neotethys it is critical to determine the specific environment of lithosphere generation. The following model (Fig. 8) considers not only the geochemical and structural data, but also the geological relations to adjacent terranes.

- The rapid convergence between Eurasia and Africa, due to the opening of the south Atlantic in the Early Cretaceous, resulted in a compressional regime in the Tethyan realm. This compression caused the formation of an intra-oceanic subduction within the İzmir–Ankara branch of the Neotethys, which led to formation of a juvenile ensimatic arc (Göncüoğlu & Türeli 1993; Tüysüz *et al.* 1995) on MORB-type oceanic crust during the Cenomanian (Fig. 8a).
- The old MORB-type oceanic crust, together with trapped OIB-type volcanics and accretion prism material, was obducted onto the Tauride–Anatolide passive margin and generated the ophiolite-bearing olistostromal sediments that overlie the slope sediments of the CACC. The emplacement of ophiolitic nappes resulted in crustal thickening and early stage syncollisional granitoids (Erler & Göncüoğlu 1996). The trench rollback generated through subduction of the forearc basin resulted in the extension of the overlying forearc region and generation of SSZ-type oceanic crust by the partial melting of already depleted MORB-type lithosphere (Fig. 8b).
- Continuing convergence during the Campanian caused the complete subduction of the old oceanic slab and final collision of the trench with the buoyant margin of the CACC. This led to a switch from extension to compression in the forearc region. The new and hot SSZ-type oceanic crust is prevented from subducting and will obduct onto the CACC (Fig. 8c).
- Complete obduction of SSZ-type oceanic crust is followed by post-collisional uplift at

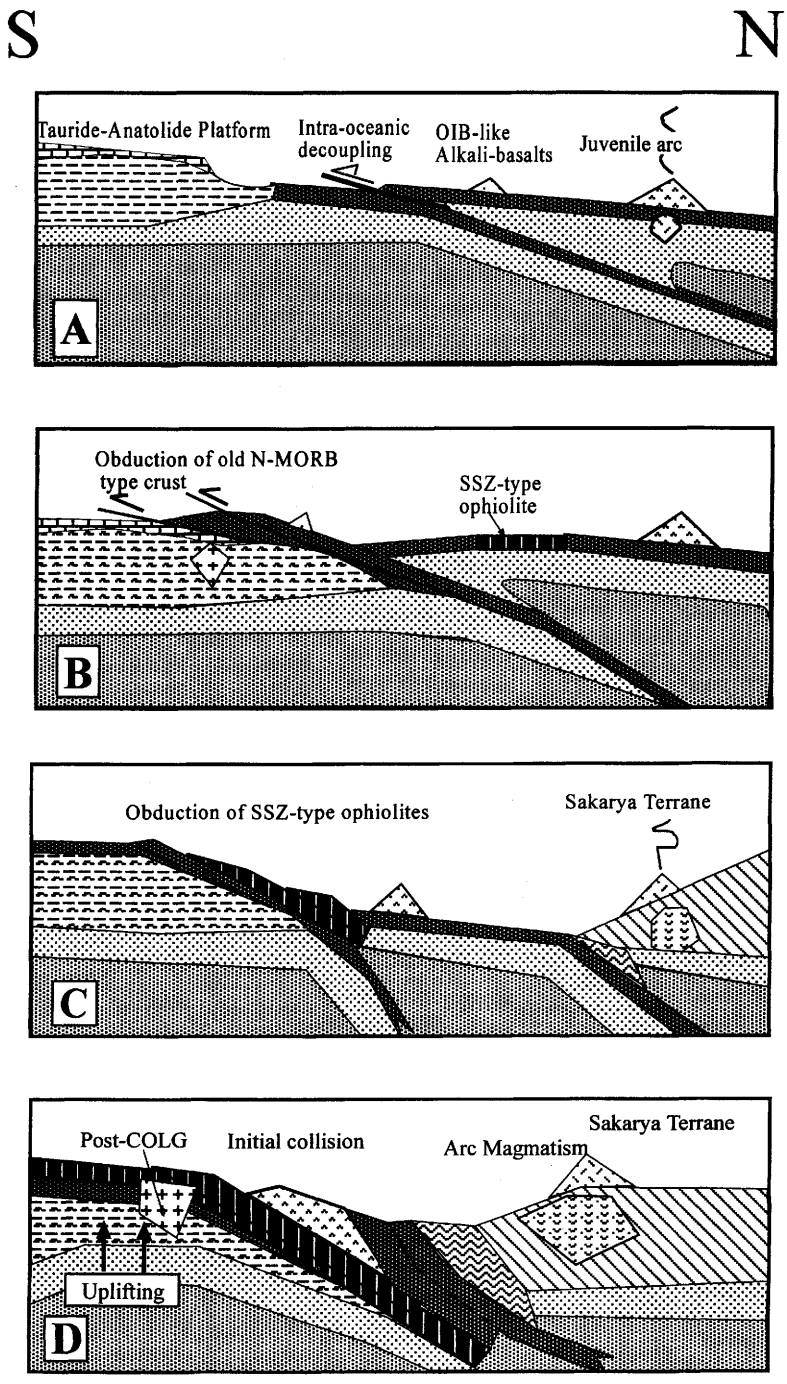

Fig. 8. Schematic representation of the tectonic evolution of the Central Anatolian ophiolites during the Late Mesozoic; (**a**) > 90 Ma: intra-oceanic decoupling within the İzmir–Ankara branch of Neotethys and the formation of an ensimatic arc; (**b**) 90–80 Ma: emplacement of old MORB-type oceanic crust onto the Tauride–Anatolide passive margin resulting in deformation and formation of SSZ-type Central Anatolian ophiolites in an arc-related setting; (**c**) 80–70 Ma: emplacement of SSZ-type ophiolites onto the CACC; (**d**) 70–65 Ma: initial collision of the arc, post-collisional extension and intrusion of post-collisional granites.

the CACC margin with Late Cretaceous post-collisional intrusions that cut both the CACC and the obducted SSZ-type ophiolites.

In conclusion, based on the geological and geochemical data, it is suggested that the fragmented Central Anatolian ophiolites, with their distinct SSZ geochemical features, were generated above an intra-oceanic subduction zone within the converging İzmir–Ankara branch of the Neotethys and emplaced southwards onto the passive margin of the CACC.

Funding for this collaborative project was provided by NATO (grant CRG 960549) and the Scientific and Research Council of Turkey (TÜBİTAK; project no. YDABÇAG-85) which are gratefully acknowledged. Analytical data production was helped by D. W. Emley and M. Aikin, Department of Earth Sciences, University of Keele, UK.

References

BECCALUVAL, L. & SERRI, G. 1988. Boninitic and low-Ti subduction-related lavas from intraocenic arc–backarc system and low-Ti ophiolites: a re-appraisal of their petrogenesis and original tectonic setting. *Tectonophysics*, **146**, 291–315.

BROUXEL, M., LECUYER, C. & LAPIERRE, H. 1989. Diversity of Magma types in a Lower Palaeozoic island arc/marginal basin system (Eastern Klamath Mountains, California, U.S.A.). *Chemical Geology*, **77**, 251–264.

COISH, R. A. 1977. Ocean floor metamorphism in the Betts Cove ophiolite, Newfoundland. *Contributions to Mineralogy and Petrology*, **60**, 255–270.

CRAWFORD, A. J., BECCALUVA, L., SERRI, G. & DOSTAL, J. 1986. Petrology, geochemistry and tectonic implications of volcanics dredged from the intersection of the Yap and Mariana trenches. *Earth and Planetary Science Letters*, **80**, 265–280.

ERDOĞAN, B., AKAY, E. & UĞUR, M. S. 1996. Geology of the Yozgat Region and evolution of the collisional Çankırı Basin. *International Geology Review*, **38**, 788–806.

ERLER, A. & GÖNCÜOĞLU, M. C. 1996. Geologic and tectonic setting of the Yozgat Batholith, Northern Central Anatolian Crystalline Complex, Turkey. *International Geology Review*, **38**, 714–726.

EWART, A., BROTHERS, R. N. & MATEEN, A. 1977. An outline of the geology and geochemistry, and the possible petrogenetic evolution of the volcanic rocks of the Tonga–Kermadec–New Zealand island arc. *Journal of Volcanology and Geothermal Research*, **2**, 205–250.

FLOYD, P. A. 1993. Geochemical discrimination and petrogenesis of alkali basalt sequences in part of the Ankara Mélange, central Turkey. *Journal of the Geological Society, London*, **150**, 541–550.

—— & CASTILLO, P. R. 1992. Geochemistry and petrogenesis of Jurassic ocean crust basalts, ODP Leg 129, Site 801. *In*: LARSON, R. & LAUNCELOT, Y. *ET AL.* (eds) *Proceedings of ODP, Scientific Results*, **129**, 361–388.

——, YALINIZ, M. K. & GÖNCÜOĞLU, M. C. 1998*a*. Geochemistry and petrogenesis of intrusive and extrusive ophiolitic plagiogranites, Central Anatolian Crystalline Complex, Turkey. *Lithos*, **42**, 225–241.

——, WINCHESTER, J. A., GÖNCÜOĞLU, M. C., YALINIZ, M. K. & PARLAK, O. 1998*b*. Geochemical overview and relations of metabasites from the Central Anatolian Crystalline Complex. *Proceedings of the Third International Turkish Geology Symposium*, METU–Ankara, Abstracts, 171.

GÖNCÜOĞLU, M. C. 1981. Origin of the viridine–gneiss in the Niğde Massif. *Geological Society of Turkey Bulletin*, **24**, 45–51.

—— 1986. Geochronological data from the southern part (Niğde Area) of the Central Anatolian Massif. *Mineral Research and Exploration Institute of Turkey (MTA) Bulletin*, **105/106**, 83–96.

—— & TÜRELI, K. 1993. Petrology and geodynamic setting of plagiogranites from Central Anatolian Ophiolites (Aksaray, Turkey). *Turkish Journal of Earth Sciences*, **2**, 195–203.

——, TOPRAK, V., ERLER, A. & KUŞCU, İ. 1991. *Geology of western Central Anatolian Massif, Part I, southern areas*. Turkish Petroleum Corporation (TPAO), Report No. 2909 [in Turkish].

GÖRÜR, N., OKTAY, F. Y., SEYMEN, İ. & ŞENGÖR, A. M. C. 1984. Palaeotectonic evolution of Tuz Gölü Basin complex, central Turkey. *In*: DIXON, J. E. & ROBERTSON, A. H. F. (eds) *The Geological Evolution of the Eastern Mediterranean*. Geological Society, London, Special Publications, **17**, 81–96.

HAWKESWORTH, C. J., GALLAGHER, K., HERGT, J. M. & MCDERMOTT, F. 1993. Mantle and slab contributions in arc magma. *Annual Reviews of Earth and Planetary Sciences*, **1**, 175–204.

——, O'NIONS, R. K., PANKHURST, R. J., HAMPTON, P. J. & EVENSEN, N. M. 1977. A geochemical study of island-arc and back-arc tholeiites from the Scotia Sea. *Earth and Planetary Science Letters*, **36**, 253–267.

HICKEY, R. L. & FREY, F. A. 1981. Rare-earth element geochemistry of Mariana fore-arc volcanics: Deep-Sea Drilling Project Site 458 and Hole 459B. *Initial Reports of the Deep-Sea Drilling Project*, **60**, 735–741.

HUMPHRIS, S. E. & THOMPSON, G. 1978*a*. Hydrothermal alteration of oceanic basalts by seawater. Geochimica et Cosmochimica Acta, **42**, 107–125.

—— & —— 1978*b*. Trace element mobility during hydrothermal alteration of oceanic basalts. *Geochimica et Cosmochimica Acta*, **42**, 127–136.

KAY, R. W. 1977. Geochemical constraints on the origin of Aleutian magmas. *In*: TALWANI, M. & PITMAN, W. C. (eds) *Island Arcs, Deep Sea Trenches and Back-Arc Basins*. American Geophysical Union, Washington, DC, 229–242.

KETIN, İ. 1959. Uber Alter und Art der kristallinen Gesteine und Erzlagerstatten in Zentral-Anatolien. *Berg und Hüttenmaennschen Monatshefte*, **104**, 163–169.

MCCULLIOCH, M. T. & GAMBLE, J. A. 1991.

Geochemical and geodynamical constraints on subduction zone magmatism. *Earth and Planetary Science Letters*, **102**, 358–374.

OKAY, A. İ., HARRIS, N. B. W. & KELLEY, S. P. 1998. Exhumation of blueschists along a Tethyan suture in northwest Turkey. *Tectonophysics*, **285**, 275–299.

PEARCE, J. A. 1975. Basalt geochemistry used to investigate past tectonic environments on Cyprus. *Tectonophysics*, **25**, 41–67.

—— 1982. Trace element characteristics of lavas from destructive plate boundaries. *In*: THORPE, R. S. (ed.) *Andesites: Orogenic Andesites and Related Rocks*. John Wiley, Chichester, 525–548.

—— 1983. Role of the subcontinental margins. *In*: HAWKESWORTH, C. J. & NORRY, M. J. (eds) *Continental Basalts and Mantle Xenoliths*. Shiva Publishing, Nantwich, 230–249.

—— & CANN, J. R. 1973. Tectonic setting of basic volcanic rocks determined using trace element analyses. *Earth and Planetary Science Letters*, **19**, 290–300.

—— & NORRY, M. J. 1979. Petrogenetic implications of Ti, Zr, Y, and Nb variations in volcanic rocks. *Contributions to Mineralogy and Petrology*, **69**, 33–47.

—— & PARKINSON, I. J. 1993. Trace element models for mantle melting: applications to volcanic arc petrogenesis. *In*: PRICHARD, H. M., ALABASTER, T., HARRIS, N. B. W. & NEARY, C. R. (eds) *Magmatic Processes and Plate Tectonics*. Geological Society, London, Special Publications, **76**, 373–403.

——, LIPPARD, S. J. & ROBERTS, S. 1984. Characteristics and tectonic significance of suprasubduction zone ophiolites. *In*: KOKELAAR, B. P. & HOWELLS, M. F. (eds) *Marginal Basin Geology*. Geological Society, London, Special Publications, **16**, 77–94.

ROBERTSON, A. H. F. & DIXON, J. E. 1984. Introduction: aspects of the geological evolution of the eastern Mediterranean. *In*: DIXON, J. E & ROBERTSON, A. H. F. (eds) *The Geological Evolution of the Eastern Mediterranean*. Geological Society, London, Special Publications, **17**, 1–74.

SAUNDERS, A. D. & TARNEY, J. 1984. Geochemical characteristics of basaltic volcanism within back-arc basin. *In*: KOKELAAR, B. P. & HOWELLS, M. F. (eds) *Marginal Basin Geology*. Geological Society, London, Special Publications, **16**, 59–76.

——, MARSH, N. G. & WOOD, D. A. 1980. Ophiolites as ocean crust or marginal basin crust: a geochemical approach. *In*: PANAYIOTOU, A. (ed.) *Ophiolites*. Proceedings of an International Symposium – 1979, Cyprus. Cyprus Geological Survey Department, 193–204.

ŞENGÖR, A. M. C. & YILMAZ, Y. 1981. Tethyan evolution of Turkey: a plate tectonic approach. *Tectonophysics*, **75**, 181–241.

SHERVAIS, J. W. 1982. Ti–V plots and the petrogenesis of modern and ophiolitic lavas. *Earth and Planetary Science Letters*, **59**, 101–118.

SMITH, R. E. & SMITH, S. E. 1976. Comments on the use of Ti, Zr, Y, Sr, K, P and Nb in classification of basaltic magmas. *Earth and Planetary Science Letters*, **32**, 114–120.

SUN, S. S. & MCDONOUGH, W. F. 1989. Chemical and isotopic systematics of oceanic basalts: implications for mantle composition and processes. *In*: SAUNDERS, A. D. & NORRY, M. J. (eds) *Magmatism in Ocean Basins*. Geological Society, London, Special Publications, **42**, 313–345.

TÜYSÜZ, O., DELLALOĞLU, A. A. & TERZİOĞLU, N. 1995. A magmatic belt within the Neo-Tethyan suture zone and its role in the tectonic evolution of northern Turkey. *Tectonophysics*, **243**, 173–191.

WHITE, W. M. & PATCHETT, P. 1984. Hf–Nd–Sr and incompatible element abundances in island arcs: implications for magma origins and crust–mantle evolution. *Earth and Planetary Science Letters*, **67**, 167–185.

WINCHESTER, J. A. & FLOYD, P. A. 1977. Geochemical discrimination of different magma series and their differentiation products using immobile elements. *Chemical Geology*, **20**, 325–343.

WOOD, D. A. 1980. The application of a Th–Hf–Ta diagram to problems of tectonomagmatic classification and to establishing the nature of crustal contamination of basaltic lavas of the British Tertiary volcanic province. *Earth and Planetary Science Letters*, **50**, 11–30.

——, JORON, J. L. & TREUIL, M. 1979. A re-appraisal of the use of trace elements to classify and discriminate between magma series erupted in different tectonic settings. *Earth and Planetary Science Letters*, **45**, 326–336.

YALINIZ, M. K. 1996. *Petrology of the Sarıkaraman Ophiolite (Aksaray–Turkey)*. PhD Thesis, Middle East Technical University.

—— & GÖNCÜOĞLU, M. C. 1998. General geological characteristics and distribution of the Central Anatolian Ophiolites. *Hacettepe University Earth Sciences*, **20**, 1–12.

——, FLOYD, P. A. & GÖNCÜOĞLU, M. C. 1996. Suprasubduction zone ophiolites of central Anatolia: geochemical evidence from the Sarıkaraman ophiolite, Aksaray, Turkey. *Mineralogical Magazine*, **60**, 697–710.

——, PARLAK, O., ÖZKAN-ALTINER, S. & GÖNCÜOĞLU, M. C. 1997. Formation and emplacement ages of supra-subduction-type ophiolites in Central Anatolia; Sarıkaraman Ophiolites, Central Turkey. *Proceedings of the Çukurova University, 20th Annual of Geological Education*, Adana, Abstracts, 61–62.

YILMAZ-ŞAHİN, S. & BOZTUĞ, D. 1997. Petrography and whole rock chemistry of the gabbroic, monzogranitic and syenitic rocks from the Çiçekdağ region, N Kirşehir, Central Anatolia, Turkey. *In*: BOZTUĞ, D., YILMAZ-ŞAHİN, S., OTLU, N. & TATAR, S. (eds) *Alkaline Magmatism, Theoretical Considerations and a Field Excursion in Central Anatolia. Proceedings*. TÜBİTAK-BAYG/NATO-D Program-Cumhuriyet University Publication, 29–42.